

Phosphate and Fluoride Processing Options for Hanford Sludge

July 2023

Amy M Westesen
Abigail M Robb
Nicholas L Cappella
Christian Alvarez
Reid A Peterson

DISCLAIMER

This report was prepared as an account of work sponsored by an agency of the United States Government. Neither the United States Government nor any agency thereof, nor Battelle Memorial Institute, nor any of their employees, **makes any warranty, express or implied, or assumes any legal liability or responsibility for the accuracy, completeness, or usefulness of any information, apparatus, product, or process disclosed, or represents that its use would not infringe privately owned rights.** Reference herein to any specific commercial product, process, or service by trade name, trademark, manufacturer, or otherwise does not necessarily constitute or imply its endorsement, recommendation, or favoring by the United States Government or any agency thereof, or Battelle Memorial Institute. The views and opinions of authors expressed herein do not necessarily state or reflect those of the United States Government or any agency thereof.

PACIFIC NORTHWEST NATIONAL LABORATORY
operated by
BATTELLE
for the
UNITED STATES DEPARTMENT OF ENERGY
under Contract DE-AC05-76RL01830

Printed in the United States of America

Available to DOE and DOE contractors from
the Office of Scientific and Technical
Information,
P.O. Box 62, Oak Ridge, TN 37831-0062
www.osti.gov
ph: (865) 576-8401
fox: (865) 576-5728
email: reports@osti.gov

Available to the public from the National Technical Information Service
5301 Shawnee Rd., Alexandria, VA 22312
ph: (800) 553-NTIS (6847)
or (703) 605-6000
email: info@ntis.gov
Online ordering: <http://www.ntis.gov>

Phosphate and Fluoride Processing Options for Hanford Sludge

July 2023

Amy M Westesen
Abigail M Robb
Nicholas L Cappella
Christian Alvarez
Reid A Peterson

Prepared for
the U.S. Department of Energy
under Contract DE-AC05-76RL01830

Pacific Northwest National Laboratory
Richland, Washington 99354

Summary

A potential strategy to stage the startup of the Hanford High-Level Waste (HLW) Vitrification Facility using an alternative option of direct feed of tank waste to the facility is being evaluated. Key processing functions previously captured during baseline pretreatment operations include leaching and washing prior to solids concentration and should be considered in the potential direct feed flowsheets to maximize waste feed loading, minimize HLW volume, and mitigate corrosion challenges associated with vitrification of high phosphate and fluoride concentrations. The effectiveness and efficiency of sludge washing can have a substantial impact on DST space and mission duration.

Two target species that benefit significantly from washing are phosphate and fluoride. Commonly present in many high-level wastes at Hanford, phosphate and fluoride are found predominately in the form of salt precipitates and can have adverse and detrimental effects on glass waste loading (Tilanus et al. 2017). Additionally, fluoride produces melter off-gas that creates corrosion risks in the off-gas system piping (Mahoney et al. 2020). Determining the solubilities of fluoride and phosphate salts, as well as the dissolution kinetics under potential HLW processing conditions will help to mitigate future operational risks and mature flowsheet technical bases.

Testing found that dissolution of phosphate and fluoride solids can be achieved under some potential processing conditions, but complete removal of the phosphate and fluoride will require some modification of the planned feed preparation process (either lower solids retrieval or use of alternative retrieval solutions). All samples washed with process water resulted in complete phosphate dissolution. Additionally, the measured solubility from AN-106 tank waste samples were consistent with the expected relationship between sodium, fluoride, and phosphate.

Acknowledgments

The authors thank Emily Campbell for conducting the technical review of this report, Dave MacPherson for his QA review and support, and Matt Wilburn for his technical editing contribution on this report. The authors also greatly appreciate Cassie Martin, Chrissy Charron, and Melanie Chiaradia for their consistent and persistent help with documenting project records and applying project standards to this work.

Contents

Summary	ii
Acknowledgments	iii
1.0 Introduction	5
2.0 Experimental	6
2.1 Simulant Preparation	6
2.2 Phosphate/Fluoride Dissolution Tests	10
2.4 Natrophosphate Solubility	11
3.0 Results	12
3.1 X-ray Diffraction (XRD) of Natrophosphate Solids	12
3.2 Dissolution Tests	12
4.0 Summary and Conclusions	16
5.0 References	17

Figures

Figure 1 Tank AN-106 Sludge Segments	6
Figure 2 Phosphate and Fluoride Solubility	11
Figure 3 XRD of Natrophosphate Solids	12
Figure 4 Phosphate/Fluoride Concentrations in the Supernate after 120 hours 25 °C	13
Figure 5 Phosphate and Fluoride Dissolution Behavior	14
Figure 6 AN-106 Solubility with 10 and 15 wt% 3.5 M Na Simulant Wash	15
Figure 7 Expected Phosphate Solubility for 3.8 M Na Simulant and AN-106 Samples	15

Tables

Table 1 Sludge Simulant Matrix	7
Table 2 Supernate Simulant Composition	7
Table 3 Reagents used for Simulant Preparation	8
Table 4 Component Masses for Matrix 1, Matrix 2, and 3.8 M Na Simulant Preparations in 100 mL volume	8
Table 5 Matrix 1, Matrix 2, and 3.8 M Na Simulants Calculated and Measured Compositions	9
Table 6 Phosphate/Fluoride Dissolution Test Matrix	10
Table 8 Phosphate and Fluoride Solubility Results	13

1.0 Introduction

Directly feeding sludge solids to the high-level waste HLW Vitrification Facility represents an alternative flowsheet seeking to initiate sludge processing as soon as possible while retaining some key processing functions outlined in the baseline treatment oriented towards maximum waste feed loading, minimization of HLW volume, and minimization of potential corrosion of the melters. In addition to the single-shell tank (SST) retrievals and waste transfers to double-shell tanks (DSTs), the direct feed flowsheet would likely benefit from some level of leaching, washing, and solids concentration, which could occur in a new facility or potentially in DSTs. At this time, these direct feed operations solely support an evaluation of potential options, with no implementation decision made.

Due to the expected high cost of HLW immobilization and geologic disposal, pretreatment processes should be implemented to reduce the volume of immobilized HLW. Phosphate (PO_4^{3-}) and fluoride (F^-) can contribute substantially to the amount of carrier fluid needed for dissolution, and the resulting volume of liquid generated. The solubility of both fluoride and phosphate salts per volume solvent decreases when the solvent is a supernatant already containing dissolved sodium salts. In addition to solubility limits, there may be kinetics constraints on the rate of dissolution. Kinetic limitations on reaching equilibrium could require more water to achieve effective dissolution rates.

Initial planning for start-up of the HLW facility has focused on treating waste in the Southeast quadrant of the Hanford site, focusing primarily on the DSTs and the sludge they contain. At this time, the primary source of sludge in the SE quadrant is in tanks AN-101 and AN-106. These two tanks represent roughly 50% of the volume of sludge present in the SE quadrant. The waste in those tanks consisted primarily of original PUREX cladding, which was high in gibbsite solids, and waste from the bismuth phosphate process (Colburn and Peterson 2020). The waste generated from the bismuth phosphate process is under scrutiny for this assessment. A recent set of samples were taken from these tanks to provide chemical and physical characterization of the solids residing in the tanks. These samples represent a type of stratigraphy of the tanks. Sampling suggests there are layers in these tanks, particularly in AN-106, that contain very high concentrations of natrophosphate ($\text{Na}_7(\text{PO}_4)_2\text{F}\cdot 19\text{H}_2\text{O}$) with some segments containing more than 50 wt% natrophosphate. Leaving this salt as part of the feed to the HLW vitrification facility will result in significantly higher glass production rates, as well as potential issues associated with processing such high phosphate concentrations. This work directly relates to potential direct feed sludge washing operations and seeks to better understand and predict the rate and extent of phosphate and fluoride salt dissolution to maximize HLW loading for phosphate or fluoride-inhibited wastes.

2.0 Experimental

All tests were conducted using simulants mimicking tank waste conditions found in AN-106. Phosphate and fluoride solubility were determined by washing a 40 wt% slurry with various amounts of process water, 1 M NaOH, or 3.8 M NaOH simulant to remove excess Na and soluble waste components. This section describes the experimental methods that were used in simulant development and dissolution experiments.

2.1 Simulant Preparation

Sample evaluation from the highest solid segments from tank AN-106 determined insoluble phosphate concentrations range from 13 wt% to 27 wt% (Hanford Best Basis Inventory). These segments account for over 70% of the insoluble phosphate in tank AN-106 and present operational challenges associated with the processing of these high phosphate layers. Figure 1 shows the sludge segment chemistry from BBI converted into wt% for tank AN-106. Particular segments of concern are 16LH, 19UH, 19LH, and 20UH due to substantial amounts (>30 wt%) natrophosphate ($\text{Na}_7(\text{PO}_4)_2\text{F}\cdot 19\text{H}_2\text{O}$) layers. Omitting clarkeite (a uranium oxide mineral), the average composition of these 4 segments is shown in Table 1 and served as the basis for the simulant sludge used in the testing reported herein.

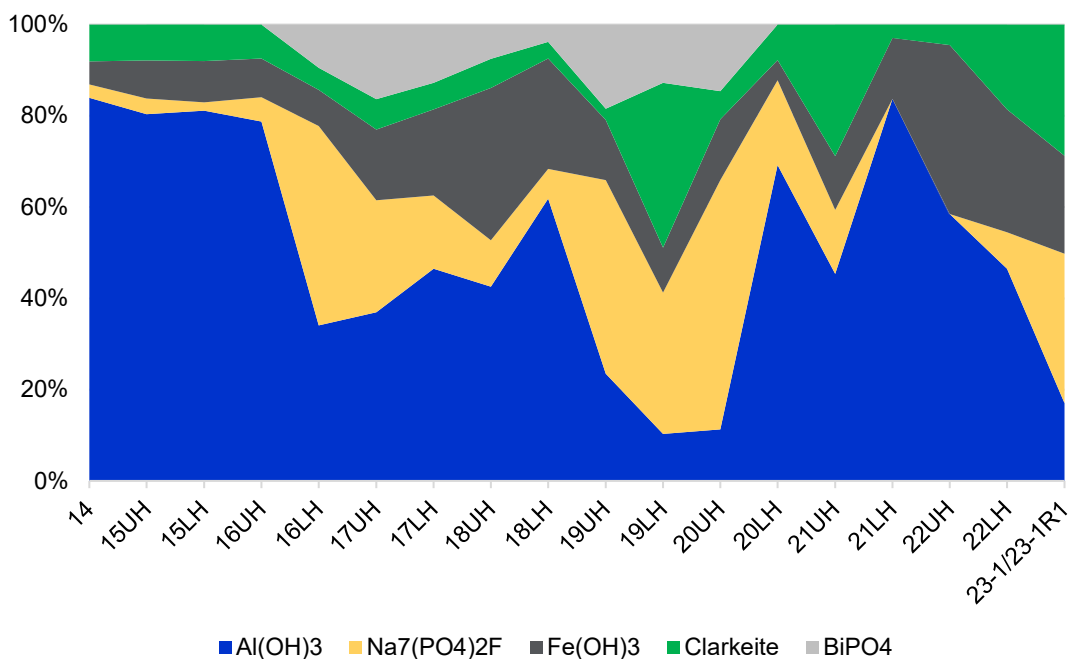


Figure 1 Tank AN-106 Sludge Segments

Table 1 Sludge Simulant Matrix

Component	MW, g/mole	Target Wt%
Na ₇ (PO ₄) ₂ F•19(H ₂ O)	712.16	47.5
BiPO ₄	303.95	15.0
Fe(OH) ₃	109.89	10.0
Al(OH) ₃	78.00	27.5

The natrophosphate was prepared by mixing equal ratios of 0.9 M NaF with 0.9 M Na₃PO₄. The latter solution was prepared at 50 °C to prevent precipitation. The two solutions were combined and chilled to 8 °C using a Benchmark (Sayreville, New Jersey) Incu-Shaker™ refrigerated orbital shaker set to 100 rpms. Solids began to form within minutes after the solutions were combined and after 2 hours the slurry was filtered. The composition of the solid phase was verified as natrophosphate using X-ray diffraction (XRD). The remaining sludge constituents were prepared from American Chemical Society (ACS) reagent grade materials.

Two supernate matrices, prepared to match the AN-106 supernate at segment layers 20UH and 16LH (as reported by BBI), bounded the high phosphate and fluoride concentrations found in tank AN-106. Table 2 shows the supernate concentrations of the segment layers alongside the target matrix concentrations used in this testing. The aluminum concentration was dropped to 0.02 M to maintain solubility in 0.1 M NaOH.

Table 2 Supernate Simulant Composition

Component	20UH, M ^a	Matrix 1 Target, M	16LH, M ^a	Matrix 2 Target, M
Fluoride	0.02	0.02	0.16	0.16
Nitrite	0.74	0.78	0.88	1.00
Nitrate	0.23	0.27	0.66	0.34
Phosphate	0.15	0.15	0.02	0.05
Hydroxide	0.10	0.10	0.10	0.10
TIC (carbonate)	0.66	0.70	0.48	0.70
Aluminum	0.01	0.02	0.20	0.02
Sodium	3.06	2.90	3.80	2.90

^a Hanford Best Basis Inventory download 3/3/23 AN-106 Tank Chemistry

The Matrix 1 and Matrix 2 simulants were mixed to achieve a 40 wt% slurry using the sludge simulant from Table 1 to represent the settled solids condition of tank AN-106 as it currently exists on the Hanford site. Aliquots of approximately 1 g of the simulant sludge were weighed into 20-mL glass vials along with 1.5 g of Matrix 1 or Matrix 2 simulant. The 40 wt% slurries then underwent washing in three dilution matrices (Columbia River process water, 1 M NaOH, and 3.8 M Na simulant) to achieve target slurry concentrations of 5, 10, and 15 wt%. The concentration of analytes in the 3.8 M Na simulant mimicked analyte concentrations from tank AP-101 and was used to represent a diluted tank waste supernate that could potentially blend with slurry feeds going to HLW.

All simulants were prepared from ACS reagent grade materials shown in Table 3 and according to a test instruction.¹ Component masses were measured into volumetric flasks containing part of the requisite deionized water. Table 4 show the added salt quantities and order of addition. After all salts were added and dissolved, the solution was brought to volume with deionized water. All densities were measured in the preparation volumetric flask at room temperature, ~20 °C (see Table 4). Each solution was passed through a 0.45-micron pore size nylon filter 24 hours after preparation to remove any precipitated components. The densities were remeasured and agreed with the pre-filtered solution density within expected uncertainty.

Table 3 Reagents used for Simulant Preparation

Compound	MW, g/mole	Manufacturer	Lot Number
Al(NO ₃) ₃ •9H ₂ O	375.13	Sigma-Aldrich	BCBR0256V
50% NaOH	40.00	Sigma-Aldrich	4102497307
KF	58.09	Thiokol Ventron	020180
NaNO ₂	69.00	Sigma-Aldrich	MKBV1410V
NaNO ₃	84.99	Sigma-Aldrich	BCBK9624V
Na ₃ PO ₄ •12H ₂ O	380.12	Fisher	126469
Na ₂ CO ₃	105.98	Sigma-Aldrich	1003143649

Table 4 Component Masses for Matrix 1, Matrix 2, and 3.8 M Na Simulant Preparations in 100 mL volume

Compound	Matrix 1 Simulant, g	Matrix 2 Simulant, g	3.8 M Na Dilution Matrix, g	1 M NaOH, g
Al(NO ₃) ₃ •9H ₂ O	0.75	0.75	9.38	--
50% NaOH	0.80	0.80	6.40	7.83
KF	0.12	0.93	0.17	--
NaNO ₂	5.38	6.90	6.21	--
NaNO ₃	1.78	2.38	10.62	--
Na ₃ PO ₄ •12H ₂ O	5.70	1.90	0.38	--
Na ₂ CO ₃	7.42	7.42	4.24	--
Density	1.133	1.144	1.186	1.126

¹ Westesen AM. 2023. TI-APD-004, *Phosphate Solubility with Washing*. Pacific Northwest National Laboratory, Richland, Washington. Not publicly available. Implemented February-March 2023.

Table 5 provides the calculated and measured component concentrations for the Matrix 1, Matrix 2, and 3.8 M Na Dilution simulants. A sample of each simulant was submitted to the Southwest Research Institute (SwRI) under Requisition # 754079 for anion analysis by ion chromatography (F^- , NO_2^- , NO_3^- , and PO_4^{3-}), and Al, Na, and P analysis by inductively coupled plasma optical emission spectroscopy (ICP-OES). The calculated concentrations for all components except aluminum in the 3.8 M Na simulant were considered definitive. Because loss of aluminum was possible during simulant preparation, the measured concentration was expected to be the definitive value.

Table 5 Matrix 1, Matrix 2, and 3.8 M Na Simulants Calculated and Measured Compositions

Simulant >>	Matrix 1 Simulant		Matrix 2 Simulant		3.8 M Na Dilution Matrix	
	Calculated Molarity	Measured Molarity	Calculated Molarity	Measured Molarity	Calculated Molarity	Measured Molarity
Al ⁺	0.02	0.02	0.02	0.02	0.25	0.02
OH ⁻	0.10	NM	0.10	NM	0.80	NM
F ⁻	0.02	0.02	0.16	0.14	0.03	0.02
NO ₂ ⁻	0.77	0.80	1.00	1.05	0.90	0.94
NO ₃ ⁻	0.21	0.27	0.28	0.34	1.25	2.01
PO ₄ ³⁻	0.15	0.15	0.05	0.04	0.01	0.01
CO ₃ ²⁻	0.70	NM	0.70	NM	0.40	NM
Na ⁺	2.9	3.01	2.9	3.09	3.8	3.82

2.2 Phosphate/Fluoride Dissolution Tests

The dissolution tests were evaluated as shown in Table 7. The 40 wt% slurries, prepared to represent current AN-106 settled solids concentration, were washed with the various wash matrices to achieve a 5, 10, or 15 wt% insoluble solids concentration. The process water was Columbia River water passed through a 0.45-micron pore size nylon filter. The density of the water was measured in a 10-mL Class A volumetric flask and an analytical balance at an ambient temperature of 22 °C and resulted in a value of 1.017 g/mL.

The 18 prepared dissolution samples were agitated at 25 °C in a Benchmark (Sayreville, New Jersey) Incu-Shaker™ set to 400 rpm for 120 hours. Aliquots (2-mL) were collected from the dissolution samples using a pipette. Aliquots were filtered through a 0.45-micron pore size nylon syringe filter to remove any solids. The weight of the known volume of each filtered sample was used to determine the density.

Table 6 Phosphate/Fluoride Dissolution Test Matrix

Parent Solution	Wash Solution	Resulting Wt% Insoluble Solids	
Matrix 1, 40 wt% insoluble solids	Process Water	5	
		10	
		15	
	1 M NaOH	5	
		10	
		15	
	3.8 M Na Simulant	5	
		10	
		15	
	Matrix 2, 40 wt% insoluble solids	Process Water	5
			10
			15
1 M NaOH		5	
		10	
		15	
3.8 M Na Simulant		5	
		10	
		15	

2.4 Natrophosphate Solubility

The equilibrium solubility of natrophosphate determines the maximum amount of fluoride and phosphate that can enter the solution (at the period of time required to approach equilibrium). The solubility expression for natrophosphate $[(Na_7F(PO_4)_2) \cdot 19H_2O]$ is

$$c_{Na}^7 c_F c_{PO_4}^2 c_{H_2O}^{19} = \frac{K_{NFP}}{\gamma_{Na}^7 \gamma_F \gamma_{PO_4}^2 \gamma_{H_2O}^{19}} \quad (1)$$

Where c_i is the molal concentration (mol/kg water in solution) of species i , γ_i is the activity coefficient of species i at the solution composition and temperature, and K_{NFP} is the solubility constant of natrophosphate at the solution temperature.

Natrophosphate is a congruent salt (Herting et al. 2002), meaning that when water is added to the pure salt, the Na:F:PO₄ ratios will be the same in the liquid (when it reaches equilibrium) as in the salt solid. In Eq. (1), the solubility product is expressed in terms of each species activities. The activity for each species is defined as the product of its concentration and its activity coefficient. The activity coefficients are functions of both temperature and interactions with every species that is present, with each species potentially having a different effect based on its concentration, charge, and other properties. The common-ion effects are driven predominantly by the left-hand side of the equation and the exponents to which concentrations are raised, though activity coefficients also play a part. For natrophosphate, the common-ion effect of sodium is very strong because sodium concentration is raised to an exponent of 7.

Figure 2 shows the directly observable solubility of product $c_{PO_4}^2$ as a function of c_F for experimental data in 3.5 M Na. Dissolution samples in this study are anticipated to start at the initial concentration in the wash matrix and increase in concentration via dissolution of the sludge solids until saturation concentrations are met, as indicated by the arrow shown in Figure 2.

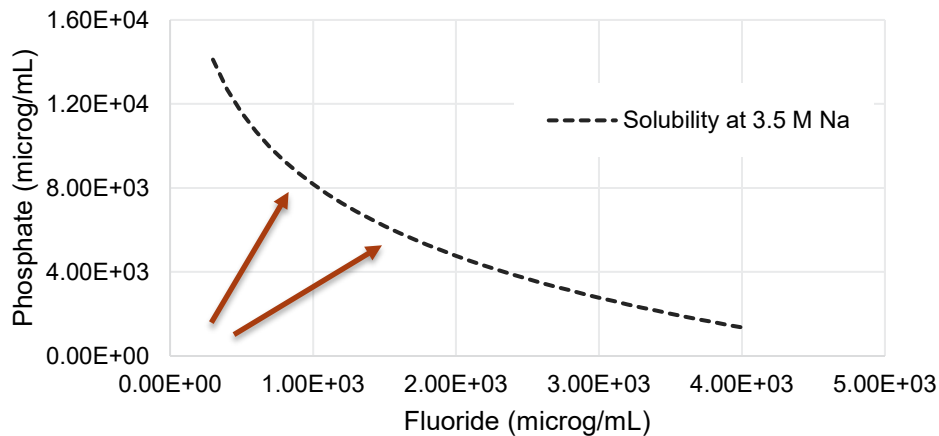


Figure 2 Phosphate and Fluoride Solubility

3.0 Results

3.1 X-ray Diffraction (XRD) of Natrophosphate Solids

XRD patterns as a function of 2θ based on $\text{CuK}\alpha$ radiation ($\lambda=1.5406 \text{ \AA}$) were measured to characterize the synthesized natrophosphate starting material for use in the dissolution tests. The calculated and observed background subtracted XRD patterns for the starting material are shown in Figure 3. Natrophosphate was the only crystalline solid phase identified by XRD. The observed diffraction pattern is displayed in black with the fit pattern to natrophosphate shown in blue. Overall fit pattern is shown in red, and a difference plot displayed in gray.

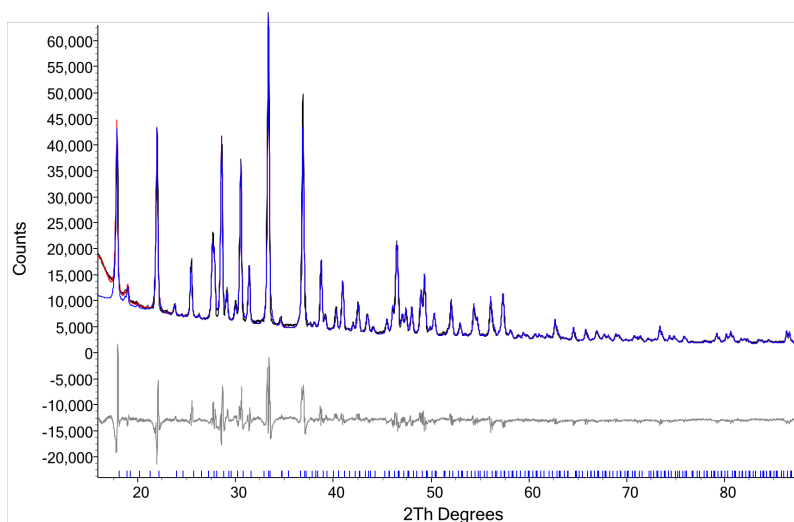


Figure 3 XRD of Natrophosphate Solids

3.2 Dissolution Tests

Tests of the solubility of phosphate and fluoride as determined by dissolution of the solid (i.e., from undersaturation) were conducted in three wash matrices. The tests were performed at ambient temperature ($25 \text{ }^\circ\text{C}$) with measurements of the concentrations of Na, PO_4 , and F taken after 120 hours. Results of the concentrations for each wash matrix are shown in Figure 4. Increasing initial wt % solids from 5 to 15 wt% increased the amount of phosphate and fluoride in solution after contacting for 120 hours.

Complete saturation of F was achieved for all wash conditions starting with Matrix 1 as the parent solution. Three testing conditions with Matrix 2 exceeded both the PO_4 and F solubility limits with the dissolved solids percentage $<100\%$, shown in Table 8; the 15 wt% solutions washed in 1 M NaOH and the 10 and 15 wt% solutions washed with 3.8 M Na simulant. When averaged, matrix 1 and 2 samples at 10 and 15 wt% washed with the 3.8 M Na simulant had nominally 45 and 31% of the PO_4 and 59% and 41% of the F dissolved from the solids, respectively. Matrix 2, prepared with significantly more F and less PO_4 , resulted in a decrease in the amount of PO_4 dissolved at the 10 and 15 wt% conditions. The same impact was seen for F dissolution in Matrix 1, which was prepared with significantly higher PO_4 than F. In regard to direct feed operations, these results also indicate that washing with 1 M NaOH to 15 wt% or a dilute (3.8 M Na) supernate stream at slurries $>10 \text{ wt\%}$ will not dissolve all the available phosphate and fluoride and would require either a more dilute slurry feed or washing with another more dilute solution.

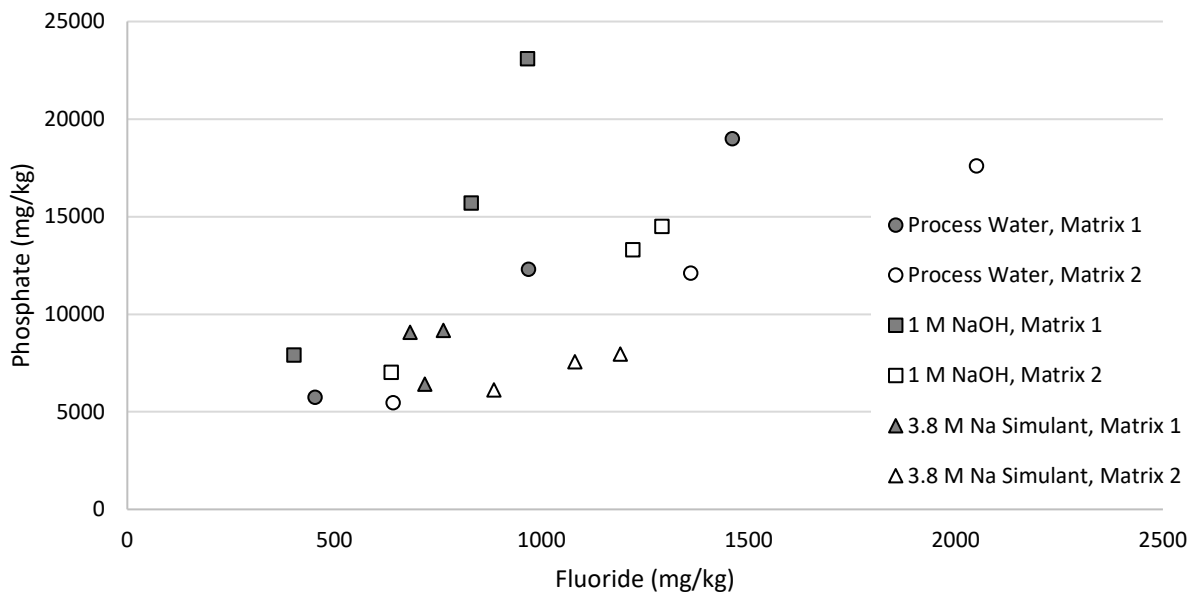


Figure 4 Phosphate/Fluoride Concentrations in the Supernate after 120 hours 25 °C

Table 7 Phosphate and Fluoride Solubility Results

Parent Solution	Wash Solution	Washed Insoluble Solids, wt%	% PO ₄ Dissolved from Solids	% F Dissolved from Solids
Matrix 1	Process Water	5	65.7%	71%
		10	69.5%	76%
		15	70.8%	76%
	1 M NaOH	5	90.7%	63%
		10	131.4%	76%
		15	58.4%	43%
	3.8 M Na Simulant	5	68.2%	82%
		10	49.2%	48%
		15	31.7%	30%
Matrix 2	Process Water	5	64.7%	102%
		10	68.6%	102%
		15	66.4%	101%
	1 M NaOH	5	80.0%	97%
		10	82.8%	97%
		15	49.9%	58%
	3.8 M Na Simulant	5	66.3%	107%
		10	41.2%	69%
		15	29.7%	52%

A general trend can be seen for the overall phosphate and fluoride dissolution in Figure 5. This figure utilizes the same data in Figure 4, with subtraction of phosphate and fluoride present as feed in the contact matrix. The solids concentration (5-15%) had minimal impact on the amounts of phosphate and fluoride dissolved when washing in process water. Similarly, washing in 1 M NaOH for slurries 5-10 wt% saw little impact in the amount of phosphate and fluoride dissolved. Interestingly, solutions with higher initial phosphate resulted in a higher fraction of the phosphate dissolved and conversely, higher initial fluoride resulted in a higher fraction of fluoride released from the solids. One possible explanation is the dissolution of the natrophosphate solids and potential re-precipitation of single salts.

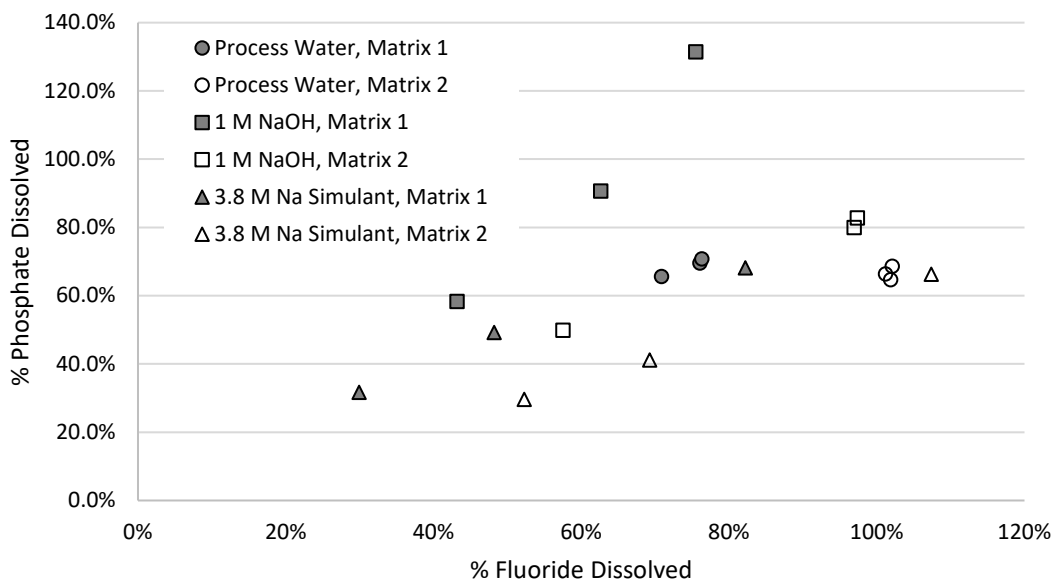


Figure 5 Phosphate and Fluoride Dissolution Behavior

The phosphate and fluoride concentrations from individual segments in tank AN-106 can be used to develop a solubility curve at the nominal sodium concentration of 3.52 M Na, shown in Figure 6. The measured concentrations show phosphate solubility decreases substantially as the fluoride concentration in the solution increases. As the only comparable condition at these Na molarities to reach solubility from the dissolution testing reported herein, the 10 and 15 wt% solutions washed with 3.8 M Na have been added to this chart. There is excellent agreement between the solubility limits calculated in this testing and those reported in the tank waste segments. This data shows the solubility sensitivity of both phosphate and fluoride in solutions containing both ions.

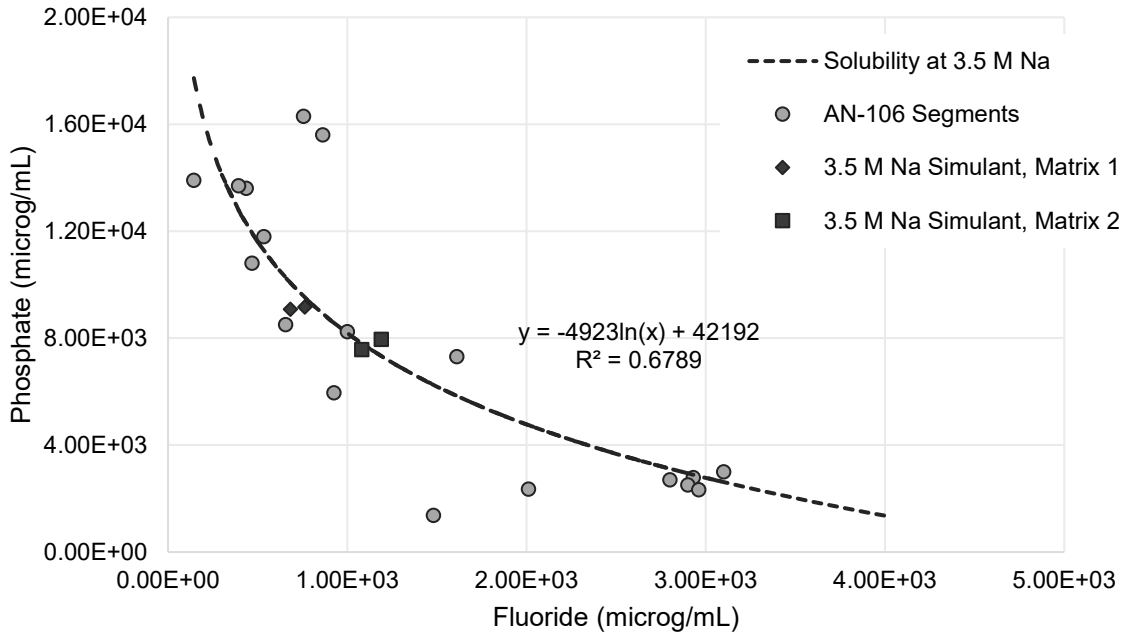


Figure 6 AN-106 Solubility with 10 and 15 wt% 3.5 M Na Simulant Wash

Comparison of solubility products (K_{sp}) using the expected solubility, shown in Eq. (2), is displayed in Figure 7.

$$K_{sp} = [Na^+]^7[F^-][PO_4^{3-}]^2 \tag{2}$$

Data from the saturated 10 and 15 wt% solutions washed with 3.8 M Na simulant along with AN-106 data show consistency with the expected solubility equation. The AN-106 data presented were selected from layers containing >5 wt% natrophosphate to ensure the solubility constraints from the double salt are present in the supernate concentrations.

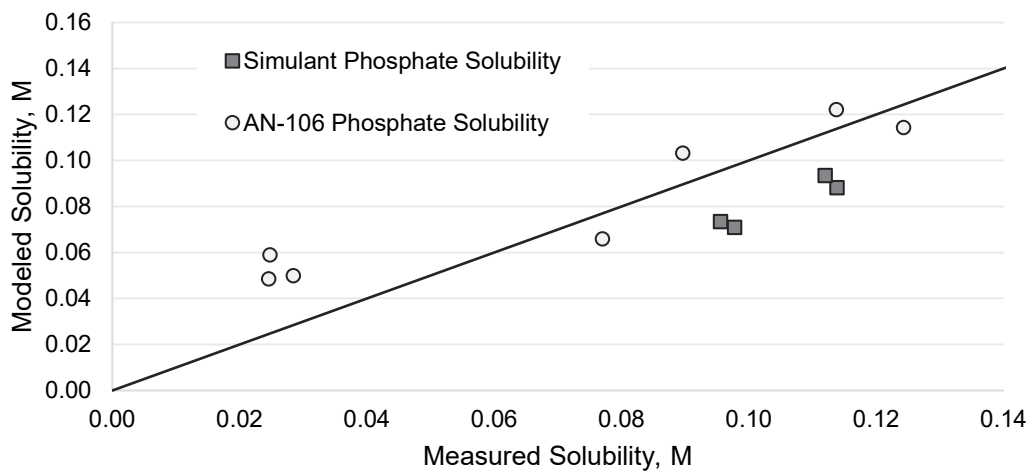


Figure 7 Expected Phosphate Solubility for 3.8 M Na Simulant and AN-106 Samples

4.0 Summary and Conclusions

The direct feed strategy represents an alternative flowsheet seeking to initiate the startup of the HLW Facility. Including some level of leaching and washing to the solid's concentration function of sludge pretreatment would have a substantial impact on DST space, mission duration, and the amount of HLW glass produced. It is well established that phosphate and fluoride compounds pose a concern for Hanford HLW glass loading as well as potential corrosion of the off-gas streams to the melter. To establish a defensible technical basis for including sludge washing in direct feed operations, phosphate and fluoride dissolution studies at potential HLW processing conditions have been explored.

Conditions mimicking the current state of Hanford tank AN-106 (40 wt% settled solids) were washed to 5, 10 and 15 wt% slurries with process water, 1 M NaOH and 3.8 M Na simulant. Ambient temperature dissolution of the samples was executed for 120 hours and the post-contacted supernate was measured for sodium, phosphate, and fluoride concentration. With process water as the solvent, full dissolution of phosphate and fluoride are achieved as well as in 1 M NaOH at 5 and 10 wt%. Slurries washed at 5 wt% with 3.8 M NaOH saw complete dissolution, however, 10 and 15 wt% slurries reached solubility limits and achieved less than 50% fluoride dissolution and nominally 60% phosphate dissolution. The 15 wt% slurries washed with 1 M NaOH also reached solubility limits.

The effectiveness of sludge washing will be dependent on multiple process options selected in support of a direct feed strategy to the HLW Facility. Based on these results, complete dissolution of phosphate and fluoride solids can be achieved under some potential processing conditions, but to remove the low solubility phosphate and fluoride salts, it will probably be necessary to use a more dilute solution than a supernate liquid as there was not sufficient dissolution at slurry concentrations above 10 wt%.

The solubility of fluoride and phosphate decreased when the solvent supernatant already contained high concentrations of dissolved fluoride or phosphate salts. Chemical analysis from AN-106 supernate showed phosphate solubility decreases substantially with increasing fluoride. Excellent agreement was seen between the solubility limits experienced in this testing and those in tank AN-106.

A direct feed flowsheet development would further benefit from conducting additional experiments to accomplish the following:

- Understanding the effect of other tank waste components responsible for increasing or decreasing the solubility of phosphate and fluoride.
- Identify the solubility limits for phosphate and fluoride at various solids loadings and in various sodium concentrations.
- Determine the effect of temperature on fluoride and phosphate solubility for natriophosphate in solutions representing plausible dissolution conditions.
- Testing with actual tank waste sludge. It is critical that testing with tank waste material be performed to verify that the observations made with the simulants are validated with actual tank waste material.

5.0 References

1. Colburn, Heather A., and Peterson, Reid A. A history of Hanford tank waste, implications for waste treatment, and disposal. United Kingdom: N. p., 2020. Web. doi:10.1002/ep.13567.
2. Herting DL, GA Cooke, and RW Warrant. 2002. Identification of Solid Phases in Saltcake from Hanford Site Waste Tanks. HNF-11585, Rev. 0, Fluor Hanford, Richland, Washington.
3. Mahoney, Lenna A., Fountain, Matthew S., and Burns, Carolyn A. M.. Dissolution of Fluoride Salts in Hanford Tank Waste. United States: N. p., 2020. Web. doi:10.2172/1645028.
4. Tank Waste Information Network System, Vol. 2023 (in series), Richland, WA, 2023.
5. Tilanus SN, LM Bergman, RO Lokken, AJ Schubick, EB West, RT Jasper, SL Orcutt, TM Holh, AN Praga, MN Wells, KW Burnett, CS Smalley, JK Bernards, SD Reaksecker, and TL Waldo. 2017. River Protection Project System Plan, ORP-11242 Rev. 8, Office of River Protection, Richland, Washington

Pacific Northwest National Laboratory

902 Battelle Boulevard
P.O. Box 999
Richland, WA 99354

1-888-375-PNNL (7665)

www.pnnl.gov